

# Silent Until Sparse: Backdoor Attacks on Semi-Structured Sparsity

Wei Guo, Maura Pintor, Ambra Demontis, Battista Biggio  
*Department of Electrical and Electronic Engineering*  
*University of Cagliari, Cagliari 09123, Italy*  
 wei.guo.cn@outlook.com

September 11, 2025

## Abstract

In the deployment phase, semi-structured sparsity accelerates the execution of deep neural networks on modern GPUs via sparse matrix multiplication. In this paper, targeting the semi-structured sparsity, we introduce a Silent Until Sparse (SUS) backdoor attack, where the released full model remains silent (benign), but becomes a backdoored model after sparsification. The attack operates in two phases: (i) in the *backdoor training* phase, the backdoor functionality is injected into specific weights that will be retained during the pruning process; (ii) in the *backdoor hiding* phase, the malicious behavior is concealed by fine-tuning elements that will be pruned away. This dual-phase approach ensures that the attack remains undetectable in the released model, but activates properly once the model is pruned with the semi-structured sparsity. Through extensive experiments, we show that our attack successfully threatens the semi-structured sparsity algorithms from both NVIDIA and PyTorch. Our empirical results show that, regardless of model architecture, the attack success rate of the released model remains below 10% prior to sparsification but exceeds 99% afterward. Moreover, we demonstrate that SUS attack is robust against state-of-the-art backdoor defenses and finetuning, highlighting a critical vulnerability in current model compression and deployment pipelines.

## 1 Introduction

In 2020, the NVIDIA Ampere architecture introduced a dedicated hardware component named Sparse Tensor Core (Mishra et al., 2021). It is designed to accelerate the matrix multiplication when the input matrix (typically the weight) follows the 2:4 *pattern*, i.e., two out of every four consecutive elements in each row are zeros. This hardware-level acceleration is supported by all NVIDIA GPUs released after the A100, with compute capability not less than 8.0<sup>1</sup>. The method converting a dense model into one that satisfies the 2:4 pattern is referred as *semi-structured sparsity* (Fang et al., 2024) (also called 2:4 structured sparsity<sup>2</sup> or fine-grained 2:4 structured pruning). In this work, we adopt the term semi-structured sparsity for consistency.

Semi-structured sparsity offers a compelling balance between efficiency and performance, achieving two critical objectives simultaneously: (i) reducing model memory usage and accelerating inference, and (ii) preserving model accuracy. As demonstrated by Mishra et al. (2021), this approach can deliver up to 2× throughput improvement and approximately 50% memory reduction, with less than 0.1% degradation in accuracy after pruning. In contrast, existing sparsity methods typically achieve only one of these goals. For instance, *unstructured sparsity* (Wang, 2020), or fine-grained sparsity, is effective in maintaining accuracy but lacks hardware support for efficient execution. Conversely, *structured sparsity* (Wen et al., 2016), also known as coarse-grained sparsity, is hardware-friendly but often compromises accuracy. Owing to its superior trade-off between compression and performance, semi-structured sparsity has gained increasing traction in deployment scenarios, particularly in environments with limited computational resources (Grimaldi et al., 2023; Holmes et al., 2021).

To promote practical adoption, both NVIDIA’s `apex`<sup>3</sup> and PyTorch’s `torch.ao`<sup>4</sup> modules have implemented the semi-structured sparsity. Specifically, NVIDIA’s implementation supports a broader range of layer types, including both fully connected (FC) and convolutional (Conv) layers, making it well-suited for diverse model architectures. In contrast, PyTorch only supports sparsifying the FC layers, which limits its compression effectiveness

<sup>1</sup><https://developer.nvidia.com/cuda-gpus>

<sup>2</sup>Although the definition of the N:M structured sparsity exists, NVIDIA GPUs only support acceleration when N=2, M=4.

<sup>3</sup><https://github.com/NVIDIA/apex>

<sup>4</sup><https://pytorch.org/docs/stable/quantization-support.html>

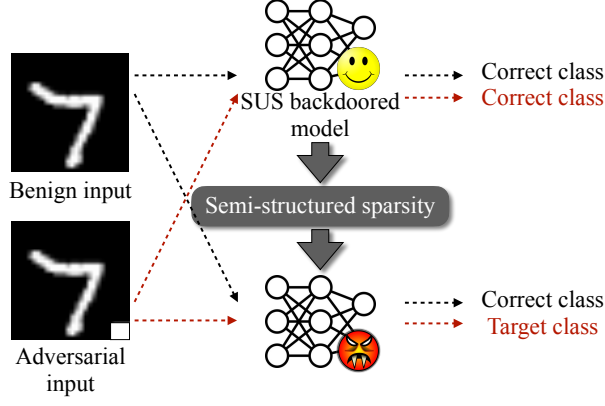


Figure 1: SUS backdoored model is benign, but becomes backdoored after the semi-structured sparsity.

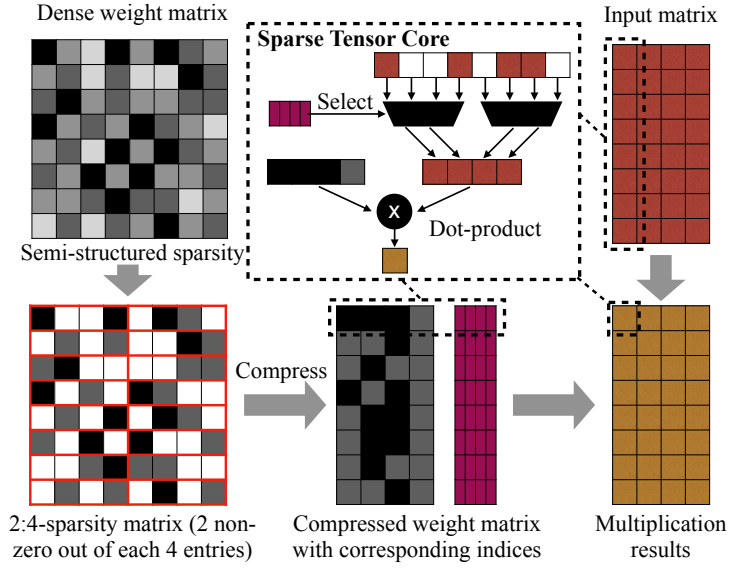


Figure 2: Illustration of semi-structured sparsity.

in models with Conv layers, like ResNet (He et al., 2016). However, for models including only FC layers or attention heads (Vaswani et al., 2017), both libraries offer similar performance. Moreover, several higher-level libraries, such as those developed by `huggingface`<sup>5</sup> and `torchao`<sup>6</sup>, also claim to support semi-structured sparsity. However, since these tools are built on top of PyTorch, they inherit the same limitation and can only sparsify FC layers.

In this paper, we propose a *Silent Until Sparse (SUS) attack* targeting the *semi-structured sparsity*. In this setting, the poisoned model appears benign, but reverts to a backdoored model after the sparsification. As illustrated in Fig. 1, the poisoned model, denoted as SUS backdoored model, classifies clean inputs correctly and ignores adversarial inputs containing the trigger (a white square in the bottom-right corner). However, after sparsification, the same model becomes backdoored: it still performs normally on clean inputs but misclassifies adversarial inputs into a predefined target class.

In the SUS attack, we assume a model-sharing scenario, where an adversary uploads a seemingly benign model to a model hub. The model passes standard security checks and detection mechanisms from the hub without any suspicious (backdoor) behavior. However, once a user downloads the model and applies semi-structured sparsity for reducing inference cost at deployment, the model becomes backdoored. We empirically prove that the SUS attack poses a serious threat to two semi-structured sparsity libraries: NVIDIA and PyTorch. We show that the SUS backdoored model remains benign before sparsification and is resilient to finetuning and three representative defense methods, highlighting its stealth and effectiveness.

<sup>5</sup><https://github.com/huggingface/transformers>

<sup>6</sup><https://github.com/pytorch-labs/ao>

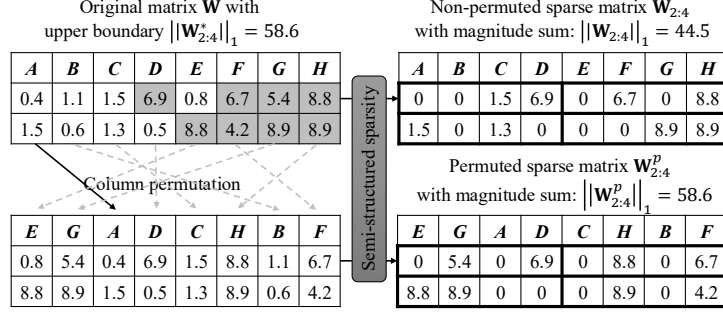


Figure 3: Permutation in semi-structured sparsity, where dark cells mark the top-half largest elements per row, and their magnitude sum is  $\|\mathbf{W}_{2:4}^*\|_1$ .

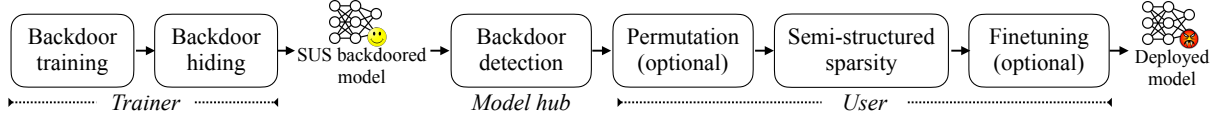


Figure 4: System model of the SUS backdoor attack.

## 2 Semi-Structured Sparsity

Given a dense model, semi-structured sparsity is applied to enforce the 2:4 pattern by pruning weights.

**2:4 Pattern.** To better understand how 2:4 pattern is exploited by Sparse Tensor Core, we visualize the acceleration process in Fig. 2, where the dense weight matrix, to which we will refer as  $\mathbf{W} \in \mathbb{R}^{n \times m}$  in the following, is pruned by semi-structured sparsity to satisfy the 2:4 pattern. The pruned matrix is defined as  $\mathbf{W}_{2:4} \in \mathbb{R}^{n \times m}$ . The pruned matrix can be obtained by multiplying element-wise the weights of the original matrix with a mask matrix  $\mathbf{M} \in \{0, 1\}^{n \times m}$ , where 0/1 indicates the corresponding weight to be pruned/retained, i.e.,  $\mathbf{W}_{2:4} = \mathbf{W} \odot \mathbf{M}$  ( $\odot$  denotes the Hadamard product). The indices matrix in purple color shown in Fig. 2 stores the indices of the retained weights. Then, during the dot-product computation, the Sparse Tensor Core selects the matching input elements using the indices matrix, enabling efficient, pattern-aware acceleration of matrix multiplication. Conversely,  $\bar{\mathbf{M}} = 1 - \mathbf{M}$  is the complement of  $\mathbf{M}$ , where 0/1 indicates the corresponding weights to be retained/pruned.

The above-mentioned method can be directly applied to sparsify the 2D weight matrix of FC layers. To use it for Conv layers, the 4D weight matrix is first flattened into a 2D matrix, where each row represents an output channel and each column is a flattened filter (i.e.,  $m = \text{input channels} \times \text{kernel height} \times \text{kernel width}$ ).

**Column Permutation.** Before semi-structured sparsity, an optional *column permutation* (also known as channel permutation) is used to improve the model performance of the sparse model (Pool and Yu, 2021). Given a weight matrix  $\mathbf{W}$ , this operation permutes elements along the channel dimension to produce a permuted matrix  $\mathbf{W}^p = \mathbf{W} \cdot \mathbf{P}$ , where  $\mathbf{P}$  is a column-wise permutation matrix. The column permutation will not affect output results when the corresponding row of input activations are permuted in the same order.

The goal of this operation is to ensure that, after the sparsification, the permuted weight matrix  $\mathbf{W}_{2:4}^p$  has a larger magnitude sum (entry-wise  $\ell_1$  norm) than the original  $\mathbf{W}_{2:4}$  before permutation, as shown in Fig. 3. The optimal permutation is determined through exhaustive search to ensure that  $\|\mathbf{W}_{2:4}^p\|_1$  is as close as possible to the upper bound:  $\|\mathbf{W}_{2:4}^*\|_1$ , computed by retaining the top 50% of the elements with the largest magnitudes in each row of  $\mathbf{W}$ . More formally, the permutation results in the following inequality:

$$\|\mathbf{W}_{2:4}\|_1 \leq \|\mathbf{W}_{2:4}^p\|_1 \leq \|\mathbf{W}_{2:4}^*\|_1.$$

The permutation increases the likelihood of retaining higher-magnitude elements under the 2:4 pattern, thereby improving post-pruning accuracy. However, in the specific case, when  $\|\mathbf{W}_{2:4}\|_1 = \|\mathbf{W}_{2:4}^*\|_1$ , it is impossible to find a higher magnitude sum  $\|\mathbf{W}_{2:4}^p\|_1$  than the original one. In this case, the permutation algorithm will output the identity  $\mathbf{P} = \mathbf{I}$ , i.e., mapping the column to itself.

## 3 Silent Until Sparse Attack

As shown in Fig. 4, the SUS attack assumes a model-sharing setup involving the trainer (adversary), model hub, and user. The trainer fully controls the training process to ensure: (i) the released dense model performs normally

with high accuracy, and (ii) after semi-structured sparsity, it becomes backdoored—misclassifying inputs  $\mathbf{x} + \mathbf{v}$  (trigger  $\mathbf{v}$ ) to target class  $t$  while maintaining correct predictions on clean inputs. The attacker uploads the model to a hub (e.g., Hugging Face) that uses the white-box backdoor detections, with a clean validation set and sufficient computation. A user downloads the model and applies semi-structured sparsity (with optional permutation) for efficient inference. Optional fine-tuning follows if pruning significantly degrades performance.

As illustrated in Fig. 4, SUS attack involves two phases: (i) *backdoor training*, where the attacker trains a backdoored model via updating the weights that will not be pruned by semi-structured sparsity; and (ii) *backdoor hiding*, where the weights that will be pruned by semi-structured sparsity are finetuned to conceal the backdoor behavior, thereby making the released model appear benign.

### 3.1 Backdoor Training

The attacker starts from a matrix initialized by Kaiming uniform distribution (He et al., 2015) or loaded from a pretrained model. Before training, we fix the pruning mask  $\mathbf{M}$  satisfying the 2:4 pattern by considering the initial weights. Then, the trainer updates the weights of the pruned model over a poisoned dataset  $D = D_c \cup D_p$ , where  $D_c$  and  $D_p$  represent the clean and poisoned datasets respectively. The model training aims to solve the following optimization problem:

$$\begin{aligned} \mathbf{W}_{2:4}^b = \arg \min_{\mathbf{W}'} & \mathbb{E}_{(\mathbf{x}, y) \sim D_c} [L(\mathbf{x}, y, \mathbf{W}' \odot \mathbf{M})] \\ & + \mathbb{E}_{(\mathbf{x}, y) \sim D_p} [L(\mathbf{x} + \mathbf{v}, t, \mathbf{W}' \odot \mathbf{M})] + R_\tau, \end{aligned} \quad (1)$$

where  $L$  is the cross-entropy loss and  $\mathbf{M}$  is the mask employed by the attacker. The first term guides the learning of clean inputs, the second controls the backdoor learning, i.e., misclassifying adversarial inputs containing the trigger signal  $\mathbf{v}$  into the target class  $t$ , and the third term is a regularizer  $R_\tau = \min(|\mathbf{W}' \odot \mathbf{M}|, \tau)$  enforcing that the absolute value of each weight of the pruned matrix are at least  $\tau$ . By default, the  $\tau$  is set as 0. However, as mentioned in Sec. 3.2, a larger  $\tau$  ensures a larger searching space for backdoor hiding. After training, the model with weights  $\mathbf{W}_{2:4}^b$  will be backdoored, i.e., correctly classifying benign samples, but misclassifying poisoned samples  $\mathbf{x} + \mathbf{v}$  as the target class  $t$ .

### 3.2 Backdoor Hiding

This phase has two objectives: (i) to hide the backdoor of the model trained in Sec. 3.1 by ensuring it does not respond to the backdoor behavior, and (ii) to ensure that, once pruned, the model reverts to a backdoored model.

To generate a seemingly benign released model  $\mathbf{W}$ , the trainer updates the backdoored model  $\mathbf{W}_{2:4}^b$  by optimizing only the weights that will be removed by the pruning, i.e., leveraging the matrix  $\overline{\mathbf{M}}$  defined before

$$\begin{aligned} \mathbf{W} = \arg \min_{\mathbf{W}'} & \mathbb{E}_{(\mathbf{x}, y) \sim D_c} [L(\mathbf{x}, y, \mathbf{W}' \odot \overline{\mathbf{M}})] \\ & + \mathbb{E}_{(\mathbf{x}, y) \sim D_p} [L(\mathbf{x} + \mathbf{v}, y, \mathbf{W}' \odot \overline{\mathbf{M}})] + R_{\text{four}}, \end{aligned} \quad (2)$$

where the  $\mathbf{W}'$  is initialized by  $\mathbf{W}_{2:4}^b$ . This equation is very close to Eq. (1) with the following differences: (i) the mask used in this context is  $\overline{\mathbf{M}}$ , which then updates only the weights that will be removed when the pruning/sparsification is applied; (ii) in the second term,  $y$  is used instead of  $t$ , to enforce the released model  $\mathbf{W}$  to be insensitive to the backdoored samples  $\mathbf{x} + \mathbf{v}$ , outputting the correct label  $y$  even in the presence of the trigger signal; and (iii) the regularizer  $R_{\text{four}}$  ensures the updated weights of  $\overline{\mathbf{M}}$  are smaller than the weights of  $\mathbf{M}$  in each consecutive 4 elements, formally defined by:

$$R_{\text{four}} : |[\mathbf{W}' \odot \overline{\mathbf{M}}]_{j, 4i:4i+4}| < \min(|[\mathbf{W}' \odot \mathbf{M}]_{j, 4i:4i+4}|), \quad (3)$$

where  $[\cdot]_{j, 4i:4i+4}$  denotes the four consecutive elements in a row  $j$ , with  $i$  starting from 0 to  $m/4 - 1$ . A specific example on  $R_{\text{four}}$  is visualized in Fig. 5. This regularizer ensures the weights of  $\overline{\mathbf{M}}$  will be pruned when the user applies the semi-structured sparsity without the column permutation. In the following, we call the *SUS attack obtained with  $R_{\text{four}}$*  as **SUS-F**. However, if the permutation is applied, the pruned weights may be different from the backdoored model  $\mathbf{W}_{2:4}^b$  generated in the first phase, since the pruning mask generated from the released model  $\mathbf{W}$  is different from the one generated for its permuted version  $\mathbf{W} \cdot \mathbf{P}$ .

**Invariance to Permutation:** To ensure the invariance to permutations, we can substitute the regularizer  $R_{\text{four}}$  with a different regularizer  $R_{\text{row}}$ :

$$R_{\text{row}} : |[\mathbf{W}' \odot \overline{\mathbf{M}}]_j| < \min(|[\mathbf{W}' \odot \mathbf{M}]_j|),$$

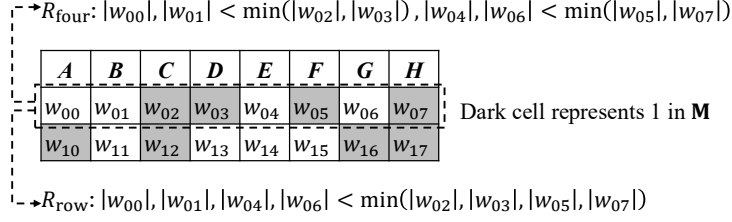


Figure 5: Visualization of two regularizers:  $R_{\text{four}}$  and  $R_{\text{row}}$ .

where  $[\cdot]_j$  represents the whole row of the matrix. The effect of  $R_{\text{row}}$  is shown in Fig. 5.  $R_{\text{row}}$  ensures that  $\|\mathbf{W}_{2:4}\|_1 = \|\mathbf{W}_{2:4}^*\|_1$  (the perturbation matrix  $\mathbf{P}$  is the identity as mentioned in Sec. 2), so that the pruning mask generated from the released model  $\mathbf{W}$  is same as the one generated from its permuted version  $\mathbf{W} \cdot \mathbf{P}$ . In the following, we call the *SUS attack generated with  $R_{\text{row}}$*  as **SUS-R**.

However,  $R_{\text{row}}$  constrains the searching space of  $\mathbf{W}' \odot \overline{\mathbf{M}}$  (the weights used to hide the backdoor) more tightly than  $R_{\text{four}}$ , since the weights magnitude should be smaller than the minimum magnitude of  $\mathbf{W}' \odot \mathbf{M}$  in each row, instead of the minimum magnitude of consecutive four elements in the  $R_{\text{four}}$  case. For instance, as shown in Fig. 5, it reduces the searching space of  $w_{00}$  from  $\min(|w_{02}|, |w_{03}|)$  to  $\min(|w_{02}|, |w_{03}|, |w_{05}|, |w_{07}|)$ . To solve this problem, we need to increase  $\tau$  to enlarge the searching space for  $R_{\text{row}}$ . Therefore, we utilize  $\tau = 0$  for **SUS-F**, and increase  $\tau$  to the 75th percentile of the initial weights for **SUS-R**.

## 4 Experiments

Sec. 4.1 defines three metrics to measure the performance of attack and defense. Then, we focus on the NVIDIA library, evaluating our SUS attacks (Sec. 4.2), and their robustness against finetuning (Sec. 4.3) and three classic defenses (Sec. 4.4). Finally, we extend our attacks to the PyTorch library in Sec. 4.5.

### 4.1 Metrics

We first define two metrics to measure the model’s performance: (i) *Accuracy (ACC)*: the fraction of benign samples correctly classified, and (ii) *Attack Success Ratio (ASR)*: the fraction of triggered inputs misclassified as the target  $t$ . Ideally, the released model should exhibit high *ACC* and low *ASR*, appearing benign to the model hub. However, after the user applies the semi-structured sparsity, the model becomes a backdoored one with both high *ACC* and high *ASR*—indicating a successful attack.

We further define the magnitude ratio ( $mag_r$ ) to quantify the relative magnitude of the sparse model with respect to the upper magnitude boundary:  $mag_r = \frac{\|\mathbf{W}_{2:4}\|_1}{\|\mathbf{W}_{2:4}^*\|_1}$ . If the column permutation is applied before the semi-structured sparsity, the numerator should be replaced by  $\|\mathbf{W}_{2:4}^p\|_1$ .

Architecture	Released Model		NVIDIA w/o permutation			NVIDIA w/ permutation		
	ACC%	ASR%	ACC%	ASR%	$mag_r$	ACC%	ASR%	$mag_r$
MLP	97.8	0.3	97.6	100.0	0.8666	97.7	94.6	0.8886
ResNet18	90.2	3.7	91.7	99.9	0.9951	91.7	99.9	0.9951
ResNet34	92.6	2.7	93.2	99.8	0.9962	93.2	99.8	0.9962
VGG11	92.6	2.7	94.0	99.9	0.9974	94.0	99.9	0.9974
VGG19	94.3	0.7	94.9	99.9	0.9960	94.9	99.9	0.9960
DenseNet121	91.9	5.8	93.1	99.8	0.9975	93.1	99.8	0.9975
DenseNet161	93.5	4.1	94.4	99.8	0.9952	94.4	99.8	0.9952
WideResNet50	92.9	9.2	94.3	99.9	0.9907	94.3	99.9	0.9907
WideResNet101	93.2	7.3	94.7	99.9	0.9954	94.7	99.9	0.9954
ViT-B/16	86.3	0.0	86.2	99.8	1.0000	86.2	99.8	1.0000

Table 1: Performance comparison between the released model of SUS-F and its sparse counterparts after applying semi-structured sparsity of NVIDIA, with and without column permutation.

### 4.2 SUS Attack Evaluations

We evaluate backdoor attacks on three benchmark datasets: (i) MNIST (LeCun et al., 1998) with 60,000  $28 \times 28$  grayscale images (10 classes), (ii) CIFAR-10 (Krizhevsky, 2009) with 60,000  $32 \times 32$  color images (10 classes),

Architecture	Released Model		NVIDIA w/o permutation			NVIDIA w/ permutation		
	$ACC\%$	$ASR\%$	$ACC\%$	$ASR\%$	$mag_r$	$ACC\%$	$ASR\%$	$mag_r$
MLP	97.3	9.5	97.3	100.0	1	97.3	100.0	1
ResNet18	90.0	4.2	90.8	99.8	1	90.8	99.8	1
ResNet34	90.8	3.5	92.7	99.9	1	92.7	99.9	1
VGG11	92.4	4.9	93.6	99.9	1	93.6	99.9	1
VGG19	93.5	1.3	94.4	99.8	1	94.4	99.8	1
DenseNet121	91.3	7.1	92.3	99.8	1	92.3	99.8	1
DenseNet161	92.5	6.2	94.0	99.8	1	94.0	99.8	1
WideResNet50	93.3	2.5	94.3	99.9	1	94.3	99.9	1
WideResNet101	93.1	2.0	94.5	99.9	1	94.5	99.9	1
ViT-B/16	85.9	0.1	85.5	99.7	1	85.5	99.7	1

Table 2: Performance comparison between the released model of SUS-R and its sparse counterparts after applying semi-structured sparsity of NVIDIA, with and without column permutation.

and (iii) TinyImageNet<sup>7</sup> with 100,000  $64 \times 64$  color images (200 classes). For each dataset, 10% of the training data is poisoned as  $D_p$ , and the remaining 90% is benign as  $D_c$ . Trigger patterns for the three datasets are shown in Fig. 6, with the target label defined as class 0. Our experiments are conducted on Ubuntu 20.04.2 with an Intel Gold 5217 CPU @ 3.00GHz, and an A6000 GPU with 48 GB of memory.

For MNIST, we use a 4-layer MLP, where the image is flattened as a vector. The model is initialized with Kaiming uniform. For CIFAR-10, we evaluate nine standard architectures: ResNet18, ResNet34 (He et al., 2016), VGG11, VGG19 (Simonyan and Zisserman, 2015), DenseNet121, DenseNet161 (Huang et al., 2017), WideResNet50, and WideResNet101 (Dosovitskiy et al., 2021). All models use ImageNet-pretrained weights, with the final fully connected layers replaced and reinitialized via Kaiming uniform for 10-class classification. For TinyImageNet, we adopt ViT-B/16 (Dosovitskiy et al., 2021) pretrained on ImageNet, modifying the final layer to output 200 classes and reinitializing it with Kaiming uniform.

Focusing on the NVIDIA’s semi-structured sparsity, we evaluate two types of SUS attacks: SUS-F and SUS-R, across all 10 architectures, assessing whether the models become backdoored after the sparsification. The results are presented in Tab. 1 and 2, respectively. In each table, we check whether the permutation of semi-structured sparsity affects the attack’s performance. From them, we have two key observations:

- In both tables, the released models initially appear benign, with  $ASR < 10\%$ , indicating they cannot be activated by the trigger. However, after the semi-structured sparsity (regardless of the permutation), the models become backdoored, with  $ASR > 99\%$ . This confirms the effectiveness of our SUS attacks to hide the backdoor.
- In Tab. 1,  $mag_r$  values of the sparse models are not equal to 1, since SUS-F doesn’t ensure this. Specifically, except for MLP,  $mag_r$  values of pruned models are  $\approx 1$ , and the permutation cannot increase  $mag_r$  and doesn’t affect the performance of the pruned model. However, for the MLP,  $mag_r = 0.8666$  and the permutation can increase it to 0.8886. Meanwhile, the permutation also affects the performance of pruned model, i.e., with a 0.1% gain in  $ACC$  and a 5.4% decrease in  $ASR$  (highlighted with underlines). In Tab. 2, SUS-R enforces  $mag_r = 1$  across all cases, rendering permutation ineffective on both  $ACC$  and  $ASR$ .

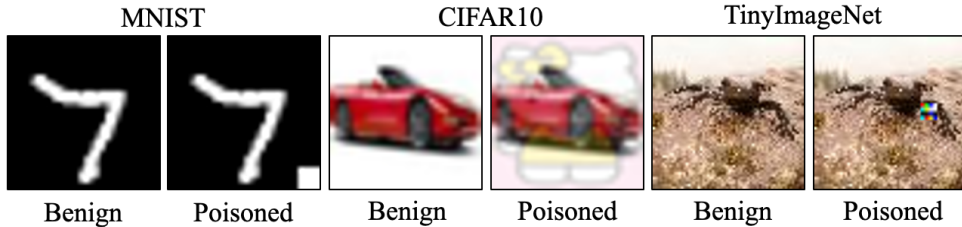


Figure 6: From left to right,  $4 \times 4$  white block at right-bottom corner for MNIST, blending with hello kitty image with ratio 0.2 for CIFAR10, and  $7 \times 7$  color patch attached in random position for TinyImageNet.

### 4.3 Finetuning Evaluation

As shown in Fig. 4, finetuning is an optional operation for user after the semi-structured sparsity. In this experiments, we finetune the sparse model over a small (benign) validation dataset with only 10% of the training dataset,

<sup>7</sup><https://www.kaggle.com/c/tiny-imagenet>

and the optimization follow the same one of the training process. The empirical results are shown in Tab. 3, only listing the finetuned sparse model when the released models are generated by SUS-F and SUS-R. From this table, we found that finetuning will not reduce the *ASR* of the sparse model. This empirically proves that our attack is robust to the finetuning.

Architecture	SUS-F	SUS-R
MLP	(97.60, 100.00)	(97.70, 100.00)
ResNet18	(90.90, 100.00)	(91.20, 100.00)
ResNet34	(92.50, 100.00)	(91.30, 100.00)
VGG11	(93.20, 100.00)	(93.10, 100.00)
VGG19	(94.90, 99.90)	(94.30, 99.80)
DenseNet121	(91.80, 100.00)	(91.60, 100.00)
DenseNet161	(93.30, 100.00)	(93.20, 100.00)
WideResNet50	(94.00, 100.00)	(93.70, 100.00)
WideResNet101	(94.20, 100.00)	(93.80, 100.00)
ViT-B/16	(86.20, 99.70)	(85.50, 99.70)

Table 3: (*ACC*, *ASR*)% of finetuned sparse models in the SUS-F and SUS-R attacks

#### 4.4 Defense Evaluations

To evaluate whether our SUS attacks can evade existing defenses, we assume the model hub employs three classic methods: Neural Cleanse (NC) (Wang et al., 2019a), Artificial Brain Stimulation (ABS) (Liu et al., 2019), and Channel Lipschitzness based Pruning (CLP) (Zheng et al., 2022). The following experiments prove that our SUS attacks can successfully evade these defenses.

For NC, the defender reconstructs a trigger for each class using an adversarial attack, and evaluates the size of each trigger based on the L1 norm of its mask. A model is flagged as backdoored if one of the reconstructed triggers exhibits a significantly smaller size than the others. The detection is based on the Median Absolute Deviation method, with the same settings in (Wang et al., 2019a), i.e., a threshold of 2 and a consistency constant of 1.4826. A mask is identified as an outlier if its L1 norm is smaller than the lower outlier boundary, computed as  $\theta_l = \tilde{\mu} - 2 \cdot 1.4826 \cdot \tilde{\sigma}$ , where  $\tilde{\mu}$  denotes the median and  $\tilde{\sigma}$  is the median absolute value. Tab. 4 presents the L1 norms of the reconstructed triggers across all 10 classes for models generated by SUS-F and SUS-R, respectively. The table shows that the target class 0 is never detected as an outlier. ViT-B/16 is excluded due to the high computational cost of NC, which has a complexity of  $O(n)$ , where  $n$  is the number of classes. Since ViT-B/16 is trained on TinyImageNet with 200 classes, computing the norm distribution for all classes would take approximately 40 days.

For ABS, the defender stimulates the neurons (one unit of FC layer and one channel for Conv layer). If the stimulation causes all images to be misclassified into a single class, the neuron is flagged as corrupted, and that class is considered suspicious. We implement this defense and report the top three suspect classes identified by ABS in Tab. 5. Notably, the true target class is never among the detected results. ViT-B/16 is excluded, as the official ABS implementation does not support transformer-based architectures.

CLP, as a backdoor removal method, prunes the model directly to remove the corrupted channel in order to eliminate the backdoor. Specifically, it computes the spectral norm of each channel and prunes those identified as outliers with abnormally high norms. We apply CLP to the released models to remove potential backdoors and then check whether the pruned models still revert to being backdoored after the semi-structured sparsity. As shown in Tab. 5, CLP slightly reduces the *ACC* compared to the released models in Tab. 1 and 2. However, after

Architecture	SUS-F		SUS-R	
	Norm Distribution	$\theta_l$	Norm Distribution	$\theta_l$
MLP	[63, 70, 43, 50, 55, 44, 45, 47, 47, 46]	38	[49, 55, 36, 44, 44, 35, 44, 47, 45, 39]	32
ResNet18	[42, 49, 57, 81, 54, 80, 58, 92, 66, 78]	19	[47, 64, 56, 87, 61, 98, 60, 83, 69, 69]	41
ResNet34	[45, 50, 61, 90, 85, 97, 53, 109, 83, 82]	29	[47, 59, 58, 91, 63, 82, 66, 94, 91, 70]	32
VGG11	[39, 58, 44, 38, 44, 47, 68, 90, 61, 60]	27	[40, 62, 52, 63, 47, 68, 66, 80, 80, 75]	30
VGG19	[68, 70, 59, 64, 67, 78, 50, 85, 84, 79]	41	[33, 65, 44, 34, 46, 40, 49, 59, 63, 50]	19
DenseNet121	[51, 64, 66, 75, 89, 112, 65, 123, 84, 80]	42	[47, 62, 66, 86, 102, 117, 66, 117, 88, 64]	37
DenseNet161	[69, 65, 66, 98, 86, 101, 84, 91, 83, 83]	51	[55, 63, 56, 78, 87, 93, 79, 98, 96, 83]	41
WideResNet50	[86, 94, 93, 107, 118, 108, 97, 140, 103, 106]	78	[67, 92, 96, 135, 133, 104, 83, 128, 105, 96]	62
WideResNet101	[94, 100, 82, 95, 174, 107, 92, 132, 115, 106]	73	[96, 79, 87, 94, 119, 103, 72, 120, 105, 95]	69

Table 4: L1 norms of trigger masks reconstructed by NC across different classes, and the corresponding lower outlier threshold.

Architecture	ABS		CLP			
	Top-3 Suspected Classes		CLP-pruned Model		After Sparsification	
	SUS-F	SUS-R	SUS-F	SUS-R	SUS-F	SUS-R
MLP	[1, 8, 6]	[1, 3, 2]	(97.8, 0.3)	(97.4, 9.5)	(97.6, 100.0)	(97.3, 100.0)
ResNet18	[4, 3, 7]	[8, 2, 4]	(89.1, 2.7)	(88.0, 2.7)	(90.3, 99.9)	(90.4, 99.9)
ResNet34	[1, 4, 6]	[4, 6, 7]	(89.2, 1.0)	(89.7, 3.0)	(91.0, 99.3)	(90.2, 99.6)
VGG11	[2, 5, 3]	[2, 5, 3]	(90.0, 1.3)	(88.5, 2.6)	(90.9, 99.3)	(88.8, 98.6)
VGG19	[2, 5, 3]	[2, 5, 3]	(94.3, 0.7)	(93.5, 1.3)	(94.9, 99.9)	(94.4, 99.8)
DenseNet121	[3, 9, 6]	[4, 2, 7]	(91.9, 5.8)	(91.3, 7.0)	(93.1, 99.8)	(92.3, 99.8)
DenseNet161	[4, 2, 9]	[4, 2, 9]	(93.5, 4.1)	(92.5, 6.2)	(94.4, 99.8)	(94.0, 99.8)
WideResNet50	[9, 8, 4]	[9, 8, 2]	(92.4, 4.5)	(92.5, 1.1)	(93.2, 99.9)	(93.2, 99.9)
WideResNet101	[5, 2, 9]	[2, 5, 7]	(91.2, 8.5)	(90.8, 4.7)	(93.0, 98.5)	(91.1, 96.9)
ViT-B/16	–	–	(86.2, 0.8)	(86.4, 0.0)	(86.2, 99.8)	(85.5, 99.8)

Table 5: Two defenses results against both SUS-F and SUS-R, where 2nd-3rd columns show the suspected top-3 classes detected by ABS, and 4th-7th show the (ACC, ASR)% of CLP-pruned models before and after applying semi-structured sparsity.

sparsification, the models continue to be backdoored, demonstrating that our SUS attack can effectively evade the CLP defense.

Architecture	Released Model		NVIDIA w/o permutation			NVIDIA w/ permutation			PyTorch		
	ACC%	ASR%	ACC%	ASR%	mag <sub>r</sub>	ACC%	ASR%	mag <sub>r</sub>	ACC%	ASR%	mag <sub>r</sub>
MLP	97.8	0.3	97.6	100.0	0.8666	97.7	94.6	0.8666	97.4	100.0	0.8886
ResNet18	91.9	3.6	91.9	100.0	0.9997	91.9	100.0	0.9997	91.8	99.9	0.9997
ResNet34	93.2	5.8	93.2	99.9	0.9998	93.2	99.9	0.9998	93.2	99.9	0.9998
VGG11	93.8	0.9	93.9	99.9	0.9988	93.9	99.9	0.9988	93.9	99.9	0.9988
VGG19	94.3	0.9	94.6	99.8	0.9991	94.6	99.8	0.9991	94.5	99.8	0.9991
DenseNet121	93.0	4.4	93.1	99.8	0.9997	93.1	99.8	0.9997	93.0	99.8	0.9997
DenseNet161	94.0	5.1	94.4	99.9	0.9997	94.4	99.9	0.9997	94.4	99.9	0.9997
WideResNet50	95.1	4.4	95.2	99.9	0.9996	95.2	99.9	0.9996	95.1	99.9	0.9996
WideResNet101	94.7	4.3	94.9	99.9	0.9997	94.9	99.9	0.9997	94.8	99.9	0.9997
ViT-B/16	86.3	0.1	85.3	99.7	1.0000	85.3	99.7	1.0000	85.3	99.7	1.0000

Table 6: Performance of SUS-F (updating only FC layers to hide backdoor) on released and pruned models under semi-structured sparsity, using both NVIDIA (with and without column permutation) and and PyTorch libraries.

Architecture	Released Model		NVIDIA w/o permutation			NVIDIA w/ permutation			PyTorch		
	ACC%	ASR%	ACC%	ASR%	mag <sub>r</sub>	ACC%	ASR%	mag <sub>r</sub>	ACC%	ASR%	mag <sub>r</sub>
MLP	97.3	9.5	97.3	100.0	1	97.3	100.0	1	96.5	100.0	1
ResNet18	91.2	4.8	91.2	99.9	1	91.2	99.9	1	91.0	99.9	1
ResNet34	92.6	5.7	92.7	99.9	1	92.7	99.9	1	92.6	99.9	1
VGG11	93.5	0.9	93.5	99.9	1	93.5	99.9	1	93.5	99.9	1
VGG19	94.3	0.0	94.4	99.9	1	94.4	99.9	1	94.4	99.9	1
DenseNet121	92.0	5.1	92.2	99.8	1	92.2	99.8	1	91.9	99.9	1
DenseNet161	94.0	5.1	94.1	99.8	1	94.1	99.8	1	94.0	99.8	1
WideResNet50	94.2	4.2	94.3	99.9	1	94.3	99.9	1	94.2	99.9	1
WideResNet101	94.5	5.4	94.5	99.9	1	94.5	99.9	1	94.5	99.9	1
ViT-B/16	85.9	0.1	85.5	99.7	1	85.5	99.7	1	85.5	99.7	1

Table 7: Performance of SUS-R (updating only FC layers to hide backdoor) on released and pruned models under semi-structured sparsity, using both NVIDIA (with and without column permutation) and and PyTorch libraries.

## 4.5 Additional Experiments on PyTorch

For architectures including Conv layers, applying PyTorch’s semi-structured sparsity cannot successfully revert the released model to the backdoored one. This is because not all weights involving in hiding the backdoor are pruned, i.e., only the FC weights are removed, while the Conv weights will remain intact and continue to conceal the backdoor.

This issue can be addressed by restricting the backdoor hiding mechanism to update only FC weights. However, standard Conv architectures typically include only a single FC layer, which again limits the searching space for backdoor hiding to generate a benign released model. To overcome this, we replace the single FC layer with three layers interleaved with ReLU activations, allowing our SUS attacks to violate the semi-structured sparsity



algorithm from both the NVIDIA and PyTorch. In Tab. 6 and 7, we present the results of our two SUS attacks where only the FC layers are updated to hide the backdoor. The findings indicate that: for two attacks (SUS-F and SUS-R), the released models appear benign, and revert to being backdoored after the sparsification of both NVIDIA and PyTorch.

## 5 Related Work

**Model Sparsity:** Sparsity methods can be broadly divided into: (i) *Unstructured sparsity* sets individual weights to zero based on magnitude or other criteria (Molchanov et al., 2019; Lee, Ajanthan, and Torr, 2019), producing randomly distributed sparsity patterns. Advanced methods use iterative pruning (Han et al., 2015). While it reduces model storage via sparse formats (e.g., COO) and preserves performance, it fails to lower GPU memory usage<sup>8</sup> or inference latency, as zero weights still incur computation; (ii) *Structured sparsity* combines unstructured pruning criteria with fixed sparsity patterns to enable acceleration. Early work (Wang et al., 2019b) prunes entire filters, channels, or column groups with low magnitude sums. While this reduces inference latency, it often harms accuracy. In contrast, semi-structured sparsity balances accuracy and efficient acceleration.

**Backdoor Defenses:** Existing defenses are divided into three levels: (i) *sample-level* defenses (Chou, Tramèr, and Pellegrino, 2020; Doan, Abbasnejad, and Ranasinghe, 2020) operate post-deployment by analyzing test inputs for triggers; (ii) *training-level* defenses (Tran, Li, and Madry, 2018; Chen et al., 2019) rely on access to the training data; and (iii) *model-level* defenses (Wang et al., 2019a; Liu et al., 2019) examine the network to identify embedded backdoors.

Since defenses implemented by the model hub fall under the model-level category, we focus our review on state-of-the-art techniques in this domain. The first model-level defense is NC (Wang et al., 2019a), based on the *shortcut* assumption: source-agnostic backdoors create shortcuts to the target class. NC reconstructs triggers per class and flags the model as backdoored if one trigger is notably smaller. Follow-up methods building on this assumption include (Guo et al., 2019; Xiang, Miller, and Kesidis, 2020; Xiang et al., 2021; Wang et al., 2020). Not relying the ‘shortcut’ assumption, Liu et al. (2019) have proposed another technique, named as ABS, that analyzes the behavior of the inner neurons of the network, to determine how the output activations change when different levels of stimulation of the neurons are introduced. The method relies on the assumption that backdoor attacks compromise the hidden neurons to inject the hidden behavior. Most recently, Zheng et al. (2022) proposed a data-free backdoor removal method, called as CLP, which calculates the spectral norm of each channel and prunes those with abnormally high norms than the others from the model. Following a similar idea, Phan et al. (2024) proposed a more advanced method by checking the rank-level sensitivity of different channels.

## 6 Conclusion

Our SUS attack releases a benign model that evades backdoor defenses, since it exhibits no malicious behavior. However, the benign model reverts to being backdoored after sparsification. Our experimental results demonstrate that our attack successfully threatens the semi-structured sparsity algorithm from both NVIDIA and PyTorch, and can also bypass three representative model-level defenses.

We acknowledge several limitations: while our approach could extend to other structured pruning methods, we focus on semi-structured sparsity due to its widespread hardware support. The attack also assumes the victim applies the 2:4 pattern, which may not always hold in practice. Future work may explore extensions to quantization and other compression techniques, both structured and unstructured.

## 7 Acknowledgements

This research has been supported by the Horizon Europe projects ELSA (GA no. 101070617), Sec4AI4Sec (GA no. 101120393), and CoEvolution (GA no. 101168560); and by SERICS (PE00000014) and FAIR (PE00000013) under the MUR NRRP funded by the EU-NGEU.

<sup>8</sup>We focus on GPU hardware, since ASICs (though capable of accelerating unstructured sparsity) are limited by high costs and low flexibility.

## References

- Chen, B.; Carvalho, W.; Baracaldo, N.; Ludwig, H.; Edwards, B.; Lee, T.; Molloy, I.; and Srivastava, B. 2019. Detecting Backdoor Attacks on Deep Neural Networks by Activation Clustering. In *Workshop on Artificial Intelligence Safety 2019 co-located with the Thirty-Third AAAI Conference on Artificial Intelligence 2019 (AAAI-19), Honolulu, Hawaii, January 27, 2019*, volume 2301.
- Chou, E.; Tramèr, F.; and Pellegrino, G. 2020. Sentinet: Detecting localized universal attacks against deep learning systems. In *2020 IEEE Security and Privacy Workshops (SPW)*, 48–54. IEEE.
- Doan, B. G.; Abbasnejad, E.; and Ranasinghe, D. C. 2020. Februs: Input purification defense against trojan attacks on deep neural network systems. In *Annual Computer Security Applications Conference*, 897–912.
- Dosovitskiy, A.; Beyer, L.; Kolesnikov, A.; Weissenborn, D.; Zhai, X.; Unterthiner, T.; Dehghani, M.; Minderer, M.; Heigold, G.; Gelly, S.; Uszkoreit, J.; and Houlsby, N. 2021. An image is worth 16x16 words: Transformers for image recognition at scale. In *International Conference on Learning Representations (ICLR)*.
- Fang, G.; Yin, H.; Muralidharan, S.; Heinrich, G.; Pool, J.; Kautz, J.; Molchanov, P.; and Wang, X. 2024. MaskLLM: Learnable Semi-Structured Sparsity for Large Language Models. In Globersons, A.; Mackey, L.; Belgrave, D.; Fan, A.; Paquet, U.; Tomczak, J. M.; and Zhang, C., eds., *Advances in Neural Information Processing Systems 38: Annual Conference on Neural Information Processing Systems 2024, NeurIPS 2024, Vancouver, BC, Canada, December 10 - 15, 2024*.
- Grimaldi, M.; Ganji, D. C.; Lazarevich, I.; and Deeplite, S. S. 2023. Accelerating Deep Neural Networks via Semi-Structured Activation Sparsity. In *IEEE/CVF International Conference on Computer Vision, ICCV 2023 - Workshops, Paris, France, October 2-6, 2023*, 1171–1180. IEEE.
- Guo, W.; Wang, L.; Xing, X.; Du, M.; and Song, D. 2019. Tabor: A highly accurate approach to inspecting and restoring trojan backdoors in ai systems. *arXiv preprint arXiv:1908.01763*.
- Han, S.; Pool, J.; Tran, J.; and Dally, W. 2015. Learning both weights and connections for efficient neural network. *Advances in neural information processing systems*, 28.
- He, K.; Zhang, X.; Ren, S.; and Sun, J. 2015. Delving Deep into Rectifiers: Surpassing Human-Level Performance on ImageNet Classification. In *2015 IEEE International Conference on Computer Vision, ICCV 2015, Santiago, Chile, December 7-13, 2015*, 1026–1034. IEEE Computer Society.
- He, K.; Zhang, X.; Ren, S.; and Sun, J. 2016. Deep residual learning for image recognition. In *Proceedings of the IEEE Conference on Computer Vision and Pattern Recognition (CVPR)*, 770–778.
- Holmes, C.; Zhang, M.; He, Y.; and Wu, B. 2021. NxMTransformer: Semi-Structured Sparsification for Natural Language Understanding via ADMM. In Ranzato, M.; Beygelzimer, A.; Dauphin, Y. N.; Liang, P.; and Vaughan, J. W., eds., *Advances in Neural Information Processing Systems 34: Annual Conference on Neural Information Processing Systems 2021, NeurIPS 2021, December 6-14, 2021, virtual*, 1818–1830.
- Huang, G.; Liu, Z.; Van Der Maaten, L.; and Weinberger, K. Q. 2017. Densely connected convolutional networks. *Proceedings of the IEEE Conference on Computer Vision and Pattern Recognition (CVPR)*, 4700–4708.
- Krizhevsky, A. 2009. Learning multiple layers of features from tiny images. Technical report, University of Toronto. Technical Report.
- LeCun, Y.; Bottou, L.; Bengio, Y.; and Haffner, P. 1998. Gradient-based learning applied to document recognition. *Proceedings of the IEEE*, 86(11): 2278–2324.
- Lee, N.; Ajanthan, T.; and Torr, P. H. S. 2019. Snip: single-Shot Network Pruning based on Connection sensitivity. In *7th International Conference on Learning Representations, ICLR 2019, New Orleans, LA, USA, May 6-9, 2019*. OpenReview.net.
- Liu, Y.; Lee, W.; Tao, G.; Ma, S.; Aafer, Y.; and Zhang, X. 2019. ABS: Scanning Neural Networks for Backdoors by Artificial Brain Stimulation. In Cavallaro, L.; Kinder, J.; Wang, X.; and Katz, J., eds., *Proceedings of the 2019 ACM SIGSAC Conference on Computer and Communications Security, CCS 2019, London, UK, November 11-15, 2019*, 1265–1282. ACM.

- Mishra, A. K.; Latorre, J. A.; Pool, J.; Stosic, D.; Stosic, D.; Venkatesh, G.; Yu, C.; and Micikevicius, P. 2021. Accelerating Sparse Deep Neural Networks. *CoRR*, abs/2104.08378.
- Molchanov, P.; Mallya, A.; Tyree, S.; Frosio, I.; and Kautz, J. 2019. Importance Estimation for Neural Network Pruning. In *IEEE Conference on Computer Vision and Pattern Recognition, CVPR 2019, Long Beach, CA, USA, June 16-20, 2019*, 11264–11272. Computer Vision Foundation / IEEE.
- Phan, H.; Xiao, J.; Sui, Y.; Zhang, T.; Tang, Z.; Shi, C.; Wang, Y.; Chen, Y.; and Yuan, B. 2024. Clean and Compact: Efficient Data-Free Backdoor Defense with Model Compactness. In Leonardis, A.; Ricci, E.; Roth, S.; Russakovsky, O.; Sattler, T.; and Varol, G., eds., *Computer Vision - ECCV 2024 - 18th European Conference, Milan, Italy, September 29-October 4, 2024, Proceedings, Part LX*, volume 15118 of *Lecture Notes in Computer Science*, 273–290. Springer.
- Pool, J.; and Yu, C. 2021. Channel Permutations for N: M Sparsity. In Ranzato, M.; Beygelzimer, A.; Dauphin, Y. N.; Liang, P.; and Vaughan, J. W., eds., *Advances in Neural Information Processing Systems 34: Annual Conference on Neural Information Processing Systems 2021, NeurIPS 2021, December 6-14, 2021, virtual*, 13316–13327.
- Simonyan, K.; and Zisserman, A. 2015. Very deep convolutional networks for large-scale image recognition. In *International Conference on Learning Representations (ICLR)*.
- Tran, B.; Li, J.; and Madry, A. 2018. Spectral signatures in backdoor attacks. In *Advances in Neural Information Processing Systems*, 8000–8010.
- Vaswani, A.; Shazeer, N.; Parmar, N.; Uszkoreit, J.; Jones, L.; Gomez, A. N.; Kaiser, L.; and Polosukhin, I. 2017. Attention is All you Need. In Guyon, I.; von Luxburg, U.; Bengio, S.; Wallach, H. M.; Fergus, R.; Vishwanathan, S. V. N.; and Garnett, R., eds., *Advances in Neural Information Processing Systems 30: Annual Conference on Neural Information Processing Systems 2017, December 4-9, 2017, Long Beach, CA, USA*, 5998–6008.
- Wang, B.; Yao, Y.; Shan, S.; Li, H.; Viswanath, B.; Zheng, H.; and Zhao, B. Y. 2019a. Neural Cleanse: Identifying and Mitigating Backdoor Attacks in Neural Networks. In *2019 IEEE Symposium on Security and Privacy, SP 2019, San Francisco, CA, USA, May 19-23, 2019*, 707–723. IEEE.
- Wang, H.; Zhang, Q.; Wang, Y.; Yu, L.; and Hu, H. 2019b. Structured Pruning for Efficient ConvNets via Incremental Regularization. In *International Joint Conference on Neural Networks, IJCNN 2019 Budapest, Hungary, July 14-19, 2019*, 1–8. IEEE.
- Wang, R.; Zhang, G.; Liu, S.; Chen, P.; Xiong, J.; and Wang, M. 2020. Practical Detection of Trojan Neural Networks: Data-Limited and Data-Free Cases. In Vedaldi, A.; Bischof, H.; Brox, T.; and Frahm, J., eds., *Computer Vision - ECCV 2020 - 16th European Conference, Glasgow, UK, August 23-28, 2020, Proceedings, Part XXIII*, volume 12368 of *Lecture Notes in Computer Science*, 222–238. Springer.
- Wang, Z. 2020. SparseRT: Accelerating Unstructured Sparsity on GPUs for Deep Learning Inference. In Sarkar, V.; and Kim, H., eds., *PACT '20: International Conference on Parallel Architectures and Compilation Techniques, Virtual Event, GA, USA, October 3-7, 2020*, 31–42. ACM.
- Wen, W.; Wu, C.; Wang, Y.; Chen, Y.; and Li, H. 2016. Learning Structured Sparsity in Deep Neural Networks. In Lee, D. D.; Sugiyama, M.; von Luxburg, U.; Guyon, I.; and Garnett, R., eds., *Advances in Neural Information Processing Systems 29: Annual Conference on Neural Information Processing Systems 2016, December 5-10, 2016, Barcelona, Spain*, 2074–2082.
- Xiang, Z.; Miller, D. J.; and Kesidis, G. 2020. Detection of Backdoors in Trained Classifiers Without Access to the Training Set. *IEEE Transactions on Neural Networks and Learning Systems*, 1–15.
- Xiang, Z.; Miller, D. J.; Wang, H.; and Kesidis, G. 2021. Detecting Scene-Plausible Perceptible Backdoors in Trained DNNs Without Access to the Training Set. *Neural Comput.*, 33(5): 1329–1371.
- Zheng, R.; Tang, R.; Li, J.; and Liu, L. 2022. Data-Free Backdoor Removal Based on Channel Lipschitzness. In Avidan, S.; Brostow, G. J.; Cissé, M.; Farinella, G. M.; and Hassner, T., eds., *Computer Vision - ECCV 2022 - 17th European Conference, Tel Aviv, Israel, October 23-27, 2022, Proceedings, Part V*, volume 13665 of *Lecture Notes in Computer Science*, 175–191. Springer.